Published in final edited form as:
J Neurosurg. 2012 August ; 117(2): 354–362. doi:10.3171/2012.5.JNS112124.

Preoperative multimodal motor mapping: a comparison of magnetoencephalography imaging, navigated transcranial magnetic stimulation, and direct cortical stimulation

Phiroz E. Tarapore, M.D.[1], **Matthew C. Tate, M.D., Ph.D.**[1], **Anne M. Findlay, M.A.**[2], **Susanne M. Honma, B.S.**[2], **Danielle Mizuiri, B.S.**[2], **Mitchel S. Berger, M.D.**[1], and **Srikantan S. Nagarajan, Ph.D.**[2]

[1]Department of Neurological Surgery, University of California, San Francisco, California

[2]Department of Radiology, University of California, San Francisco, California

Abstract

Object—Direct cortical stimulation (DCS) is the gold-standard technique for motor mapping during craniotomy. However, preoperative noninvasive motor mapping is becoming increasingly accurate. Two such noninvasive modalities are navigated transcranial magnetic stimulation (TMS) and magnetoencephalography (MEG) imaging. While MEG imaging has already been extensively validated as an accurate modality of noninvasive motor mapping, TMS is less well studied. In this study, the authors compared the accuracy of TMS to both DCS and MEG imaging.

Methods—Patients with tumors in proximity to primary motor cortex underwent preoperative TMS and MEG imaging for motor mapping. The patients subsequently underwent motor mapping via intraoperative DCS. The loci of maximal response were recorded from each modality and compared. Motor strength was assessed at 3 months postoperatively.

Results—Transcranial magnetic stimulation and MEG imaging were performed on 24 patients. Intraoperative DCS yielded 8 positive motor sites in 5 patients. The median distance ± SEM between TMS and DCS motor sites was 2.13 ± 0.29 mm, and between TMS and MEG imaging motor sites was 4.71 ± 1.08 mm. In no patients did DCS motor mapping reveal a motor site that was unrecognized by TMS. Three of 24 patients developed new, early neurological deficit in the form of upper-extremity paresis. At the 3-month follow-up evaluation, 2 of these patients were significantly improved, experiencing difficulty only with fine motor tasks; the remaining patient had improvement to 4/5 strength. There were no deaths over the course of the study.

Address correspondence to: Sri Nagarajan, Ph.D., Department of Radiology, University of California at San Francisco, 513 Parnassus Avenue, S362, San Francisco, California 94143. srikantan.nagarajan@ucsf.edu.

This article contains some figures that are displayed in color online but in black-and-white in the print edition.

Disclosure

Author contributions to the study and manuscript preparation include the following. Conception and design: Nagarajan, Tarapore. Acquisition of data: Tarapore, Tate, Findlay, Honma, Mizuiri, Berger. Analysis and interpretation of data: Nagarajan, Tarapore, Findlay, Honma, Mizuiri. Drafting the article: Tarapore. Critically revising the article: all authors. Reviewed submitted version of manuscript: all authors. Statistical analysis: Tarapore. Administrative/technical/material support: Nagarajan, Findlay, Honma, Mizuiri. Study supervision: Nagarajan, Tarapore.

Conclusions—Maps of the motor system generated with TMS correlate well with those generated by both MEG imaging and DCS. Negative TMS mapping also correlates with negative DCS mapping. Navigated TMS is an accurate modality for noninvasively generating preoperative motor maps.

Keywords

transcranial magnetic stimulation; magnetoencephalography; motor mapping; direct cortical stimulation

---

The management of brain tumors in and around the rolandic cortex presents a specific challenge to the operative neurosurgeon. The desire to resect as extensively as possible must be balanced by a constant attention to preserving a patient's existing function. Although DCS remains the gold standard for generating maps of the motor system,[10,16,35] noninvasive methods of motor mapping are becoming increasingly accurate and useful.

Magnetoencephalography imaging refers to the reconstruction of the spatiotemporal dynamics of brain sources from magnetoencephalographic data. When coregistered with an anatomical scan, such as high-resolution MRI, MEG imaging can be integrated into a neuronavigation system and provide intraoperative guidance to the surgical team.[33] Several previous studies have shown that ERD in the β frequency band (approximately 20 Hz) is associated with voluntary movement.[1,6,7,23–30,43–45] These ERDs can be interpreted as an electrophysiological correlate of activation of cortical areas involved in the production of motor behavior. Preoperative MEG imaging mapping of the motor cortex has been validated in comparison with intraoperative DCS maps, and is a useful modality for preoperative localization of this region.[14,19,21,39,40,48]

Transcranial magnetic stimulation is a noninvasive technique that can also generate preoperative motor maps. Transcranial magnetic stimulation generates a brief, powerful magnetic field that induces an action potential in a small population of neurons. When pyramidal neurons of the primary motor cortex are stimulated, the resultant action potential triggers small movements in the relevant muscle groups, which can then be detected via electromyography. Like MEG imaging, TMS can be integrated with a neuronavigation system, allowing for coregistration with an anatomical scan.[15,17,18,31] This navigated TMS system has the ability to generate motor maps of high resolution that (in 1 other series[32]) correlate well with intraoperative DCS maps.

In this study, we seek to examine the accuracy of navigated TMS for preoperative motor mapping. We compare this modality with MEG imaging, which is already well validated as a noninvasive method for preoperative mapping, and with DCS, which is the gold-standard technique. In addition to evaluating the accuracy of positive motor sites, we ascertain whether a negative TMS motor map correlates with negative maps in the other 2 modalities. Finally, we correlate these findings with clinical outcomes.

Methods

Patient Population

We prospectively enrolled 24 adult patients with brain tumors in and around the somatosensory cortex. All patients were referred for clinical MEG scanning and MEG imaging at the University of California, San Francisco, Biomagnetic Imaging Laboratory. For inclusion in the study, patients had to be scheduled for subsequent craniotomy with motor mapping. Patients with seizure frequency greater than 1 per week were excluded from the study, as were patients with cardiac pacemakers or implanted metal devices in the cranial region. All patients were treated by a single neurosurgeon (M.S.B.). Patients underwent neurological examination before and after surgery; they were followed for 3 months postoperatively, and their clinical examination results were recorded. All patients gave written informed consent to participate in the research and the study was conducted under Institutional Review Board approval.

Structural Images

High-resolution MRI was performed at 1.5-T to provide necessary anatomical detail for surgical planning and intraoperative neuronavigation. The protocol typically included the following sequences: 1) a T1-weighted, 3D, spoiled gradient–recalled acquisition in steady-state sequence with TR 34 msec, TE 3–8 msec, and flip angle 30° ; and 2) a T2-weighted, 3D fast spin echo sequence with TR 3000 msec and TE 105 msec. Both sequences used the following parameters: slice thickness 1.5 mm, matrix size 256 × 256 × (108 to – 140), and FOV 260 mm × 260 mm, with skin-to-skin coverage to include the nasion and preauricular points.

Magnetoencephalography Recordings

Magnetic fields were recorded in a magnetically shielded room using a 275-channel whole-head CTF Omega 2000 system (VSM MedTech). A sampling rate of 600 Hz was used. Each patient lay on a comfortable bed. For the motor task, individuals performed self-paced unilateral, index-finger button pressing once every 3–4 seconds for a total of 100–250 movements. The button press was used to mark the onset of movement. Motor tasks were performed using both left and right fingers.

Analysis of MEG Data

The MEG data obtained during the motor task were bandpass-filtered in the β band (15–30 Hz). Sensor data covariance was computed in a window beginning approximately 600 msec before the onset of movement, designated as the active period. Sensor data covariance was also computed for a 600-msec baseline control period 1–2 seconds after movement onset. Details of the adaptive spatial filtering algorithm used to analyze the β-band ERD are described elsewhere.[41,42,47] In brief, an estimate of the source power at each voxel in the brain, based on the MEG data, are computed for the active and control time periods, using a forward-field computed assuming a multiple local-sphere spherical volume conductor model, making use of the sensor data covariance. Source power estimates are obtained at a 5-mm resolution across the entire brain for the active and control periods, and a pseudo-F

ratio is calculated. Negative values of the pseudo-F ratio indicate desynchronization and positive values indicate synchronization. This process of adaptive spatial filtering was performed using a commercially available, synthetic-aperture magnetometry software package (VSM MedTech Ltd.) and integrated with custom-built in-house software package (NUTMEG).[8] Locations of peaks of the ERD images were used to indicate the location of the hand motor cortex. For each individual, the ERD/event-related synchronization images were overlaid on the preoperative high-resolution MR images as described above.

Transcranial Magnetic Stimulation Recordings

We used the Navigated Brain Stimulation system (Nexstim) for motor mapping of frontal cortical areas. This device delivers a biphasic magnetic pulse from a figure-of-eight coil. This magnetic pulse is able to induce an electric field; in the case of cortical stimulation, the magnetic pulse induces an electric field in the neurons beneath. The strength and directionality of this field is calculated according to a dynamic spherical model, which takes into account the preset parameters of stimulation as well as the patient's scalp/skull thickness.[37,46]

A high-resolution T1-weighted MRI series was acquired as described above and uploaded to the Navigated Brain Stimulation software, which recreated a 3D model of the patient. This anatomical scan was then coregistered to the patient's head using anatomical landmarks and surface matching.[12] The mapping surface was located between 23- and 28-mm deep to the scalp; the peeling depth was adjusted on a case-by-case basis to best reveal the cortical anatomy.

Surface electrodes (Neuroline 720, Ambu) were attached to the patient's muscles for electromyography re cording. All patients had electrodes affixed to abductor digiti quinti and abductor pollicis brevis muscles; the orbicularis oris was monitored on a case-by-case basis if warranted by tumor location. Resting motor threshold was then determined. The most likely location of the hand knob was identified. This area was then stimulated while systematically varying the location of the induced electrical field, as well as its tilt and yaw. Resting motor threshold was defined as the minimum stimulation intensity capable of generating an MEP in 50% of cases.[34]

Motor mapping was then performed at 110% of resting motor threshold. The peritumoral region was covered systematically, including the motor cortex as well as adjacent cortices. Areas adjacent to the tumor, as well as the tumor itself, were mapped if the lesion was visible at the peeling depth. The electrical field strength was optimized by the software, which dictated the tilt of the stimulator coil. The orientation of the dipole was largely maintained in perpendicularity to the adjacent sulcus. In areas that induced MEPs in target muscle groups, the density of stimulations increased so as to precisely identify the locus of maximal MEP. This locus was then identified as the "motor site."

Surgical Procedure and DCS Mapping

All patients underwent surgery for tumor resection, using DCS mapping 24 hours after the MEG scan and TMS were performed. Neuronavigation was used in all cases; the craniotomy was tailored according to the exact extension of the tumor with a 3-cm margin of

surrounding brain tissue. A positive motor site was defined as an area that induced involuntary movement when stimulated. Full details of our DCS mapping protocol have been previously described.[3,4] A bipolar electrode with 5-mm spaced tips, delivering a biphasic current, was applied to the brain; the biphasic current consisted of square-wave pulses in 4-second trains at 60 Hz, with single-pulse phase duration of 1 msec. Cortical mapping was initiated at 1.5 mA under awake surgery or 6 mA under general anesthesia, and increased to a maximum of 6 mA under awake anesthesia and 16 mA under general anesthesia. Stimulation sites were identified using sterile numbered labels distributed per square centimeter of exposed cortex. After the cortical mapping was completed, the tumor was removed in a tailored fashion; when a functional cortical site was detected, a 1-cm margin of tissue was always preserved around this site.[11] The exact locations of the functional sites were registered with a navigational MRI system; this was performed just after the cortical mapping and before any tumor removal that could have been a source of spatial mislocalization by brain shift.[13]

Analysis of Motor Sites

Intraoperative DCS motor sites were translated into DICOM coordinates. Because the MEG imaging motor site was often buried in a sulcus, a projection was made to the cortical surface so that MEG imaging motor sites would be coplanar with TMS and DCS motor sites. These sites were also translated into DICOM coordinates, along with the DCS sites, and were imported into the Navigated Brain Stimulation software. This software allows for real-time visualization of 3D reconstructions of anatomical MR images with TMS, MEG imaging, and DCS motor sites overlaid. Distances between TMS and MEG imaging sites were calculated for every patient. For patients with positive DCS sites, distances were calculated between these sites and TMS as well.

Because TMS motor maps localized abductor digiti quinti and abductor pollicis brevis muscles while MEG localized the flexor digitorum profundus muscle, the motor maps for the 2 modalities were expected to be somewhat disparate. In an effort to estimate the location of the flexor digitorum profundus muscle on TMS, the midpoint was calculated between the abductor digiti quinti and abductor pollicis brevis muscles. This point formed the basis for a secondary analysis, in which the distance between it and the MEG motor site was calculated.

Results

Demographics and Tumor Characteristics

In a 5-month period, 31 craniotomies were performed with motor mapping at the University of California, San Francisco, by a single surgeon (M.S.B.). Of these 31 patients, 5 refused participation, 1 was excluded based on tumor type (metastatic lesion), and 1 was excluded for frequent seizures, leaving 24 patients used in the analysis (Table 1). There were 10 male and 14 female patients, and ages ranged from 27 to 70 years with a median age of 41 years. Left-sided lesions were found in 18 patients, while 6 were found on the right side. Twelve patients were newly presenting and 12 had recurrence. Eight patients had frontal lesions, 7 had temporal lesions, and 5 had parietal lesions. The remaining 4 tumors spanned multiple

lobes. Final pathology results demonstrated anaplastic astrocytoma (WHO Grade III) in 4 patients, glioblastoma (WHO Grade IV) in 7 patients, oligoastrocytoma (WHO Grade II) in 5 patients, oligodendroglioma (WHO Grade II) in 4 patients, oligodendroglioma (WHO Grade III) in 3 patients, and treatment effect in 1 patient (Table 1).

Motor Mapping

All 24 patients underwent MEG imaging and TMS as described above. The MEG imaging algorithm successfully localized a motor site for index finger flexion in each patient (Fig. 1). Transcranial magnetic stimulation was able to localize abductor digiti quinti and abductor pollicis brevis muscles in 23 patients; TMS could not identify any motor sites in 1 patient with an infiltrating glioma within the somatosensory cortex (Fig. 2). Transcranial magnetic stimulation also identified a motor site for the orbicularis oris in 3 patients. Eighteen patients underwent intraoperative motor mapping with DCS, which identified 8 motor sites in 5 patients, of which 2 were thumb motor sites, 3 were little finger motor sites, and 3 were mouth motor sites (Fig. 3). The remaining patients had negative motor maps using DCS (Fig. 4). There was no significant difference in quality of motor maps by any modality between patients undergoing initial resection and those undergoing resection for recurrence.

Comparison of Motor Maps

In comparing TMS motor sites to MEG motor sites, 2 analyses were performed. The first analysis compared each patient's abductor digiti quinti and abductor pollicis brevis sites with the MEG imaging–derived motor site for index finger flexion. Orbicularis oris TMS sites were omitted because MEG imaging did not identify any mouth motor sites. In all, 46 sites from each group were compared and 46 distances were calculated. According to the Lilliefors test, the data followed a normal distribution. The median distance between MEG imaging of the index finger and TMS of the abductor digiti quinti muscle was 8.98 ± 1.41 mm; and that between MEG imaging of the index finger and TMS of the abductor pollicis brevis muscle was 6.16 ± 0.73 mm (Fig. 5). Overall, the median distance from MEG imaging of the index finger to either TMS site was 8.20 ± 0.77 mm (Fig. 6). The second analysis compared the MEG imaging index finger site with an interpolated midpoint between TMS of the abductor digiti quinti muscle and TMS of the abductor pollicis brevis muscle. In this analysis, 23 sites from each group were compared and 23 distances were calculated. The data were normally distributed. The median distance was 4.71 ± 1.08 mm (Fig. 7).

In comparing TMS with DCS motor sites, a total of 8 TMS points were compared with 8 DCS points. The TMS and DCS points were matched based on their association with the same target muscle group. With 8 points in each group, a total of 8 distances were calculated. The median distance between TMS and DCS sites was 2.13 ± 0.29 mm (Fig. 8). Finally, the median distance between MEG imaging–derived motor sites and DCS was 12.1 ± 8.2 mm. The distances among all 3 modalities are summarized in Table 2. Of note, all patients who had negative DCS mapping also had negative TMS mapping within the area subtended by the craniotomy. Stated differently, DCS mapping did not find any new motor site that TMS failed to identify.

Clinical Outcomes

No patients had significant complications during their postoperative course. Of the 24 patients in the series, 21 had intact motor strength at the time of discharge. Two of these patients experienced significant resolution of motor strength at the 3-month follow-up evaluation and were experiencing difficulty with fine motor tasks only. The remaining patient, at last follow-up of 6 months, had 4/5 strength in proximal arm muscles, as well as significant right upper-extremity apraxia and difficulty with fine motor tasks. No patients had complete palsy of any muscle group at 3 months. No patient died over the course of the study.

Discussion

Direct cortical stimulation for motor mapping in patients with tumors in proximity to sensorimotor cortex allows the surgeon to maximize the extent of resection while minimizing morbidity. Current data suggests that 3%–5% of patients undergoing this procedure will incur a new, permanent motor deficit.[5,10,16] With sensitive mapping techniques and neuronavigation, we are pushing the extent of resection to its safe perimeter. In these cases, the spatial resolution of the mapping technique is the limiting factor in demarcating the boundary between eloquent and noneloquent tissue. Preoperative motor mapping with TMS can aid in the rapid, accurate identification of these regions, allowing the surgeon to hone in on known motor sites that might otherwise be difficult to identify because of distorted anatomy. Our data suggest that the TMS motor maps are well within the tolerances described for both TMS and DCS. Similarly, the discrepancies between TMS and MEG imaging motor sites are within the tolerances described for these techniques.

Magnetoencephalography Imaging Compared With TMS Motor Sites

We and others have reported previously on the accuracy of MEG β-band ERD in localizing the hand motor cortex.[21,22] In our prior series, localization of the hand motor cortex using β-band ERD showed good correlation with DCS, with a median distance of approximately 1 cm between sites. In that series as well as the present study, the chosen motor task is a button push with the index finger. This task yields a strong signal with a focal movement, thereby optimizing the signal-to-noise ratio. Similarly, the TMS mapping is performed using optimum target muscle groups—in this case, the abductor digiti quinti and abductor pollicis brevis. In our experience, these muscles yield better electromyographic signals and, consequently, better maps than do other muscles such as the first dorsal interosseous. These differences are likely a result of anatomical limitations, as well as our usage of surface rather than needle electromyography electrodes, a choice made to optimize patient comfort. Thus, the MEG imaging and TMS motor maps are based on motor sites that, although neighbors in the somatotopic cortical rep-resentation, are not identical, and both modalities have the resolution to identify these sites as distinct.

Thus, as we report, there is a consistent distance between the MEG imaging motor site and each of the 2 TMS motor sites, which likely represents the distance between index finger and little finger/thumb sites in the somatotopic cortical representation. This finding is consistent with prior functional MRI-based studies of hand somatotopy.[2,9] It should also be

emphasized that although we designate a single motor "site" based on the point of maximal electromyographic response, we did find that the representation of a given muscle is often spread out over some area, which is consistent with prior observations of redundancy in the motor systems of primates and humans.[9,20,38] Despite the overlap in finger somatotopy, there is a relative preservation of an ordered arrangement of finger representations.[9] We therefore interpolated the midpoint between abductor digiti quinti muscle and abductor pollicis brevis muscle to predict the location of the index finger motor site. As predicted, the distance between this derived point and the MEG imaging index finger site was smaller, thereby confirming that the location of our motor sites fit with existing models of hand somatotopy.

Transcranial Magnetic Stimulation and Negative DCS Mapping

As an increasing numbers of studies[35,36] report on the safety of negative mapping, the smaller, tailored cortical exposure is rapidly becoming accepted as the standard of care for management of tumors in eloquent cortex. Two studies[5,16] have shown that patients with negative DCS maps have lower rates of postoperative deficit than patients whose cortical or subcortical motor tracts were identified. In our study, preoperative TMS mapping identified a motor site if, and only if, DCS identified that motor site. Thus, there is complete concordance between the TMS and DCS motor maps. Additionally, the agreement between TMS and MEG imaging motor maps serves as a positive control in those patients with negative DCS motor maps. Therefore, if a given craniotomy does not overlap with any positive TMS motor sites, the surgeon should expect to find a negative DCS motor map.

Limitations of the Study

As with all modalities that depend on coregistration between the patient and a prior scan, there are inherent inaccuracies in TMS neuronavigation. All of our TMS coregistrations achieved the minimum tolerance, and the manufacturer-described error in the system is 5.7 mm. Thus, the distances between TMS, DCS, and MEG imaging sites were approaching the maximum resolution attainable by the system. Despite this accuracy, in individual cases the distance between DCS and TMS motor sites was more than 2 cm. Therefore, if greater accuracy is required, DCS mapping remains essential. It should be noted that this study focused on hand motor sites, and thus its findings should not be generalized to other motor regions such as the face and legs. Furthermore, other higher-level functions (such as language) still require separate, dedicated testing. Finally, the number of patients with positive mapping sites is relatively small, and data from larger patient series must be accumulated before any alteration of clinical practice should be considered.

Despite undergoing multimodal motor mapping, 1 patient in this study developed a new, permanent postoperative deficit. In this patient, both TMS and DCS failed to find any motor sites, despite exhaustive mapping of the rolandic cortex using both modalities (MEG imaging identified 1 motor site within the lesion; Fig. 2). This case illustrates that the limitations of TMS may be similar to those of DCS. If tumor infiltration has distorted or destroyed enough pyramidal cells, then neither modality can induce an action potential in enough neurons to generate a detectable response. This situation may represent a potential way of achieving a false-negative result. Another limitation of TMS is its inability to access

subcortical regions. Thus, while it has demonstrated great promise in mapping cortical regions, the surgeon must rely on DCS for mapping deep white matter tracts after resection has begun. Finally, because TMS is based on preoperative MRI, the TMS motor map cannot account for the shifts and tissue distortion that occur intraoperatively. Again, the surgeon must use DCS to attain real-time data if it is required.

Conclusions

Maps of the motor system generated with TMS correlate well with those generated by both MEG imaging and DCS. Negative TMS mapping also correlates with negative DCS mapping. Although DCS is necessary for intraoperative motor mapping, navigated TMS is an accurate modality for noninvasively generating preoperative motor maps.

Acknowledgments

This work was supported by NIH R01 grants DC004855, DC006435, and NS67962, as well as NIH/National Center for Research Resources UCSF-CTSI grants UL1 RR024131 (to Dr. Nagarajan) and 5T32CA151022-02 (to Dr. Tarapore).

Abbreviations used in this paper

DCS	direct cortical stimulation
ERD	event-related desynchronization
MEG	magnetoencephalography
MEP	motor evoked potential
TMS	transcranial magnetic stimulation.

References

1. Babiloni C, Carducci F, Cincotti F, Rossini PM, Neuper C, Pfurtscheller G, et al. Human movement-related potentials vs desynchronization of EEG alpha rhythm: a high-resolution EEG study. Neuroimage. 1999; 10:658–665. [PubMed: 10600411]
2. Beisteiner R, Windischberger C, Lanzenberger R, Edward V, Cunnington R, Erdler M, et al. Finger somatotopy in human motor cortex. Neuroimage. 2001; 13:1016–1026. [PubMed: 11352607]
3. Berger MS, Ojemann GA. Intraoperative brain mapping techniques in neuro-oncology. Stereotact Funct Neurosurg. 1992; 58:153–161. [PubMed: 1439333]
4. Berger MS, Ojemann GA, Lettich E. Neurophysiological monitoring during astrocytoma surgery. Neurosurg Clin N Am. 1990; 1:65–80. [PubMed: 2135974]
5. Carrabba G, Fava E, Giussani C, Acerbi F, Portaluri F, Songa V, et al. Cortical and subcortical motor mapping in rolandic and perirolandic glioma surgery: impact on postoperative morbidity and extent of resection. J Neurosurg Sci. 2007; 51:45–51. [PubMed: 17571034]
6. Crone NE, Miglioretti DL, Gordon B, Lesser RP. Functional mapping of human sensorimotor cortex with electrocorticographic spectral analysis. II. Event-related synchronization in the gamma band. Brain. 1998; 121(Pt 12):2301–2315. [PubMed: 9874481]
7. Crone NE, Miglioretti DL, Gordon B, Sieracki JM, Wilson MT, Uematsu S, et al. Functional mapping of human sensorimotor cortex with electrocorticographic spectral analysis. I. Alpha and beta event-related desynchronization. Brain. 1998; 121(Pt 12):2271–2299. [PubMed: 9874480]
8. Dalal SS, Zumer JM, Agrawal V, Hild KE, Sekihara K, Nagarajan SS. NUTMEG: a neuromagnetic source reconstruction toolbox. Neurol Clin Neurophysiol. 2004; 52:2004.

9. Dechent P, Frahm J. Functional somatotopy of finger representations in human primary motor cortex. Hum Brain Mapp. 2003; 18:272–283. [PubMed: 12632465]
10. Duffau H, Capelle L, Sichez J, Faillot T, Abdennour L, Law Koune JD, et al. Intra-operative direct electrical stimulations of the central nervous system: the Salpêtrière experience with 60 patients. Acta Neurochir (Wien). 1999; 141:1157–1167. [PubMed: 10592115]
11. Haglund MM, Berger MS, Shamseldin M, Lettich E, Ojemann GA. Cortical localization of temporal lobe language sites in patients with gliomas. Neurosurgery. 1994; 34:567–576. [PubMed: 7516498]
12. Hannula H, Ylioja S, Pertovaara A, Korvenoja A, Ruohonen J, Ilmoniemi RJ, et al. Somatotopic blocking of sensation with navigated transcranial magnetic stimulation of the primary somatosensory cortex. Hum Brain Mapp. 2005; 26:100–109. [PubMed: 15864816]
13. Hill DL, Maurer CR Jr, Maciunas RJ, Barwise JA, Fitzpatrick JM, Wang MY. Measurement of intraoperative brain surface deformation under a craniotomy. Neurosurgery. 1998; 43:514–528. [PubMed: 9733307]
14. Inoue T, Shimizu H, Nakasato N, Kumabe T, Yoshimoto T. Accuracy and limitation of functional magnetic resonance imaging for identification of the central sulcus: comparison with magnetoencephalography in patients with brain tumors. Neuroimage. 1999; 10:738–748. [PubMed: 10600419]
15. Julkunen P, Säisänen L, Danner N, Niskanen E, Hukkanen T, Mervaala E, et al. Comparison of navigated and non-navigated transcranial magnetic stimulation for motor cortex mapping, motor threshold and motor evoked potentials. Neuroimage. 2009; 44:790–795. [PubMed: 18976714]
16. Keles GE, Lundin DA, Lamborn KR, Chang EF, Ojemann G, Berger MS. Intraoperative subcortical stimulation mapping for hemispherical perirolandic gliomas located within or adjacent to the descending motor pathways: evaluation of morbidity and assessment of functional outcome in 294 patients. J Neurosurg. 2004; 100:369–375. [PubMed: 15035270]
17. Krings T, Chiappa KH, Foltys H, Reinges MH, Cosgrove GR, Thron A. Introducing navigated transcranial magnetic stimulation as a refined brain mapping methodology. Neurosurg Rev. 2001; 24:171–179. [PubMed: 11778822]
18. Krings T, Foltys H, Reinges MH, Kemeny S, Rohde V, Spetzger U, et al. Navigated transcranial magnetic stimulation for presurgical planning—correlation with functional MRI. Minim Invasive Neurosurg. 2001; 44:234–239. [PubMed: 11830785]
19. Lin PT, Berger MS, Nagarajan SS. Motor field sensitivity for preoperative localization of motor cortex. J Neurosurg. 2006; 105:588–594. [PubMed: 17044563]
20. McKiernan BJ, Marcario JK, Karrer JH, Cheney PD. Corticomotoneuronal postspike effects in shoulder, elbow, wrist, digit, and intrinsic hand muscles during a reach and prehension task. J Neurophysiol. 1998; 80:1961–1980. [PubMed: 9772253]
21. Nagarajan S, Kirsch H, Lin P, Findlay A, Honma S, Berger MS. Preoperative localization of hand motor cortex by adaptive spatial filtering of magnetoencephalography data. J Neurosurg. 2008; 109:228–237. [PubMed: 18671634]
22. Pang EW, Drake JM, Otsubo H, Martineau A, Strantzas S, Cheyne D, et al. Intraoperative confirmation of hand motor area identified preoperatively by magnetoencephalography. Pediatr Neurosurg. 2008; 44:313–317. [PubMed: 18504418]
23. Pfurtscheller G. Functional brain imaging based on ERD/ERS. Vision Res. 2001; 41:1257–1260. [PubMed: 11322970]
24. Pfurtscheller G. Functional topography during sensorimotor activation studied with event-related desynchronization mapping. J Clin Neurophysiol. 1989; 6:75–84. [PubMed: 2915031]
25. Pfurtscheller G. Mapping of event-related desynchronization and type of derivation. Electroencephalogr Clin Neurophysiol. 1988; 70:190–193. [PubMed: 2456197]
26. Pfurtscheller G. Spatiotemporal analysis of alpha frequency components with the ERD technique. Brain Topogr. 1989; 2:3–8. [PubMed: 2641472]
27. Pfurtscheller G, Berghold A. Patterns of cortical activation during planning of voluntary movement. Electroencephalogr Clin Neurophysiol. 1989; 72:250–258. [PubMed: 2465128]

28. Pfurtscheller G, Lopes da Silva FH. Event-related EEG/MEG synchronization and desynchronization: basic principles. Clin Neurophysiol. 1999; 110:1842–1857. [PubMed: 10576479]
29. Pfurtscheller G, Neuper C, Berger J. Source localization using event-related desynchronization (ERD) within the alpha band. Brain Topogr. 1994; 6:269–275. [PubMed: 7946926]
30. Pfurtscheller G, Pregenzer M, Neuper C. Visualization of sensorimotor areas involved in preparation for hand movement based on classification of mu and central beta rhythms in single EEG trials in man. Neurosci Lett. 1994; 181:43–46. [PubMed: 7898767]
31. Picht T, Mularski S, Kuehn B, Vajkoczy P, Kombos T, Suess O. Navigated transcranial magnetic stimulation for preoperative functional diagnostics in brain tumor surgery. Neurosurgery. 2009; 65(6 Suppl):93–99. [PubMed: 19935007]
32. Picht T, Schmidt S, Brandt S, Frey D, Hannula H, Neuvonen T, et al. Preoperative functional mapping for rolandic brain tu mor surgery: comparison of navigated transcranial magnetic stimulation to direct cortical stimulation. Neurosurgery. 2011; 69:581–588. [PubMed: 21430587]
33. Romstöck J, Fahlbusch R, Ganslandt O, Nimsky C, Strauss C. Localisation of the sensorimotor cortex during surgery for brain tumours: feasibility and waveform patterns of somatosensory evoked potentials. J Neurol Neurosurg Psychiatry. 2002; 72:221–229. [PubMed: 11796773]
34. Rossini PM, Barker AT, Berardelli A, Caramia MD, Caruso G, Cracco RQ, et al. Non-invasive electrical and magnetic stimulation of the brain, spinal cord and roots: basic principles and procedures for routine clinical application. Report of an IFCN committee. Electroencephalogr Clin Neurophysiol. 1994; 91:79–92. [PubMed: 7519144]
35. Sanai N, Berger MS. Intraoperative stimulation techniques for functional pathway preservation and glioma resection. Neurosurg Focus. 2010; 28(2):E1. [PubMed: 20121436]
36. Sanai N, Mirzadeh Z, Berger MS. Functional outcome after language mapping for glioma resection. N Engl J Med. 2008; 358:18–27. [PubMed: 18172171]
37. Sarvas J. Basic mathematical and electromagnetic concepts of the biomagnetic inverse problem. Phys Med Biol. 1987; 32:11–22. [PubMed: 3823129]
38. Schieber MH, Hibbard LS. How somatotopic is the motor cortex hand area? Science. 1993; 261:489–492. [PubMed: 8332915]
39. Schiffbauer H, Berger MS, Ferrari P, Freudenstein D, Rowley HA, Roberts TP. Preoperative magnetic source imaging for brain tumor surgery: a quantitative comparison with intraoperative sensory and motor mapping. J Neurosurg. 2002; 97:1333–1342. [PubMed: 12507131]
40. Schiffbauer H, Berger MS, Ferrari P, Freudenstein D, Rowley HA, Roberts TP. Preoperative magnetic source imaging for brain tumor surgery: a quantitative comparison with intraoperative sensory and motor mapping. Neurosurg Focus. 2003; 15(1):E7. [PubMed: 15355009]
41. Sekihara K, Nagarajan SS, Poeppel D, Marantz A. Asymptotic SNR of scalar and vector minimum-variance beamformers for neuromagnetic source reconstruction. IEEE Trans Biomed Eng. 2004; 51:1726–1734. [PubMed: 15490820]
42. Sekihara K, Nagarajan SS, Poeppel D, Marantz A, Miyashita Y. Reconstructing spatio-temporal activities of neural sources using an MEG vector beamformer technique. IEEE Trans Biomed Eng. 2001; 48:760–771. [PubMed: 11442288]
43. Stancák A Jr, Pfurtscheller G. Desynchronization and recovery of beta rhythms during brisk and slow self-paced finger movements in man. Neurosci Lett. 1995; 196:21–24. [PubMed: 7501247]
44. Taniguchi M, Kato A, Fujita N, Hirata M, Tanaka H, Kihara T, et al. Movement-related desynchronization of the cerebral cortex studied with spatially filtered magnetoencephalography. Neuroimage. 2000; 12:298–306. [PubMed: 10944412]
45. Taniguchi M, Kato A, Ninomiya H, Hirata M, Cheyne D, Robinson SE, et al. Cerebral motor control in patients with gliomas around the central sulcus studied with spatially filtered magnetoencephalography. J Neurol Neurosurg Psychiatry. 2004; 75:466–471. [PubMed: 14966166]
46. Tarkiainen A, Liljestrom M, Seppa M, Salmelin R. The 3D topography of MEG source localization accuracy: effects of conductor model and noise. Clin Neurophysiol. 2003; 114:1977–1992. [PubMed: 14499760]

47. Vrba J, Robinson SE. Signal processing in magnetoencephalography. Methods. 2001; 25:249–271. [PubMed: 11812209]

48. Yang TT, Gallen CC, Schwartz BJ, Bloom FE. Noninvasive somatosensory homunculus mapping in humans by using a large-array biomagnetometer. Proc Natl Acad Sci U S A. 1993; 90:3098–3102. [PubMed: 8464929]

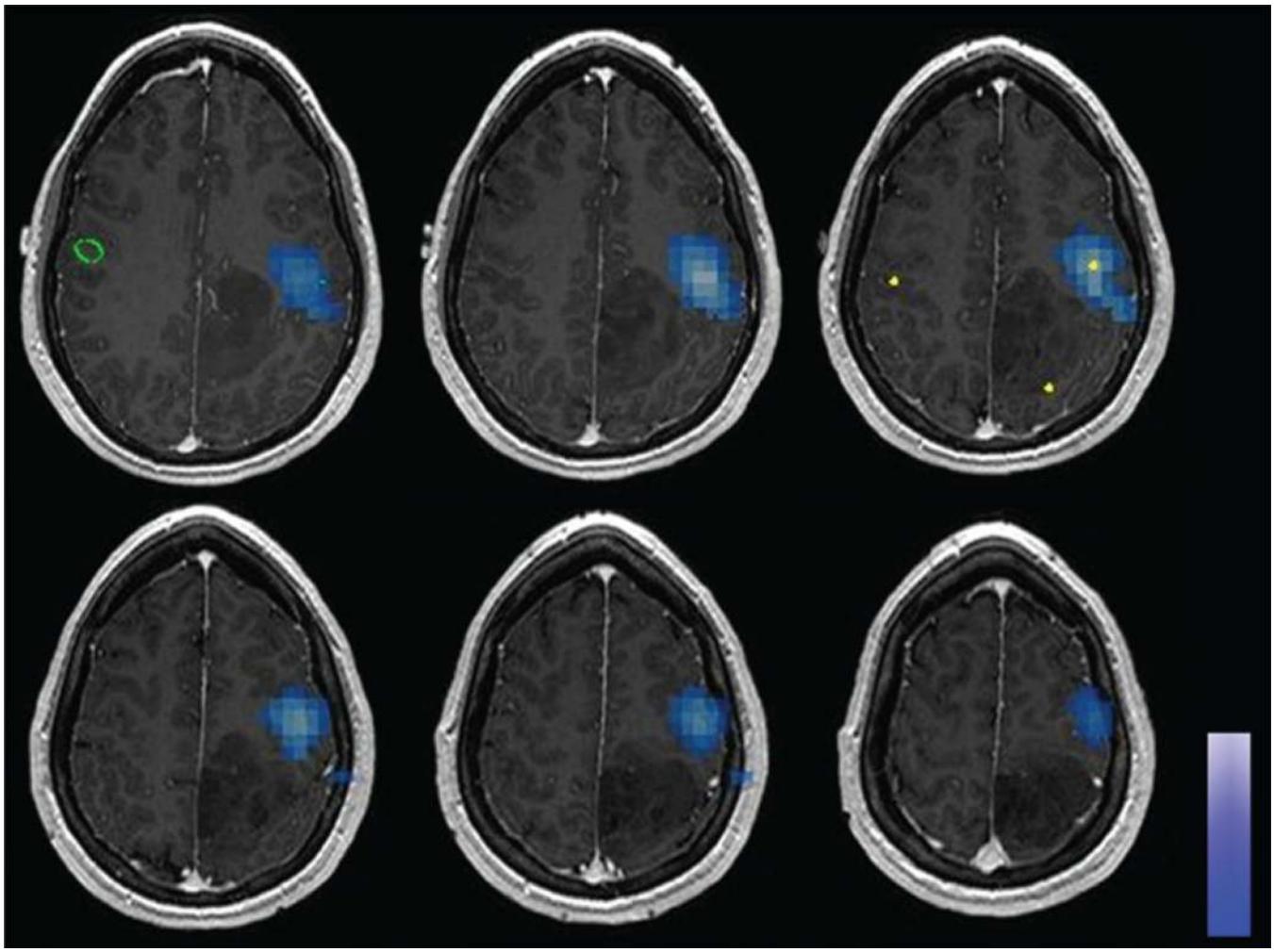

Fig. 1.

Axial MR images showing synthetic aperture magnetometry analysis of MEG imaging data in 1 patient, localizing the motor site for the index finger *(blue areas)*.

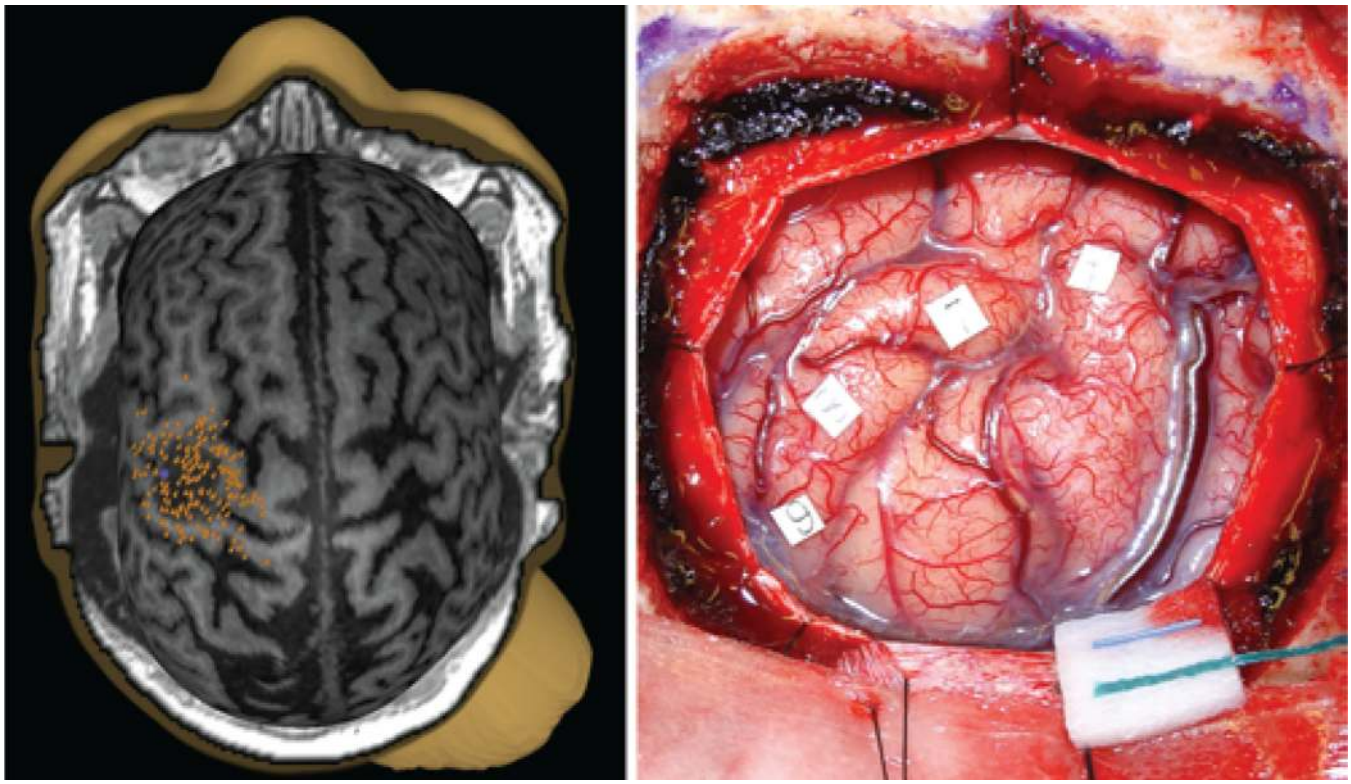

Fig. 2.

Images obtained in a patient with a tumor in the somatosensory cortex. **Left:** Transcranial magnetic stimulation map; no positive motor sites were identified. **Right:** Intraoperative photograph; *numbered squares* indicate sensory sites identified with DCS.

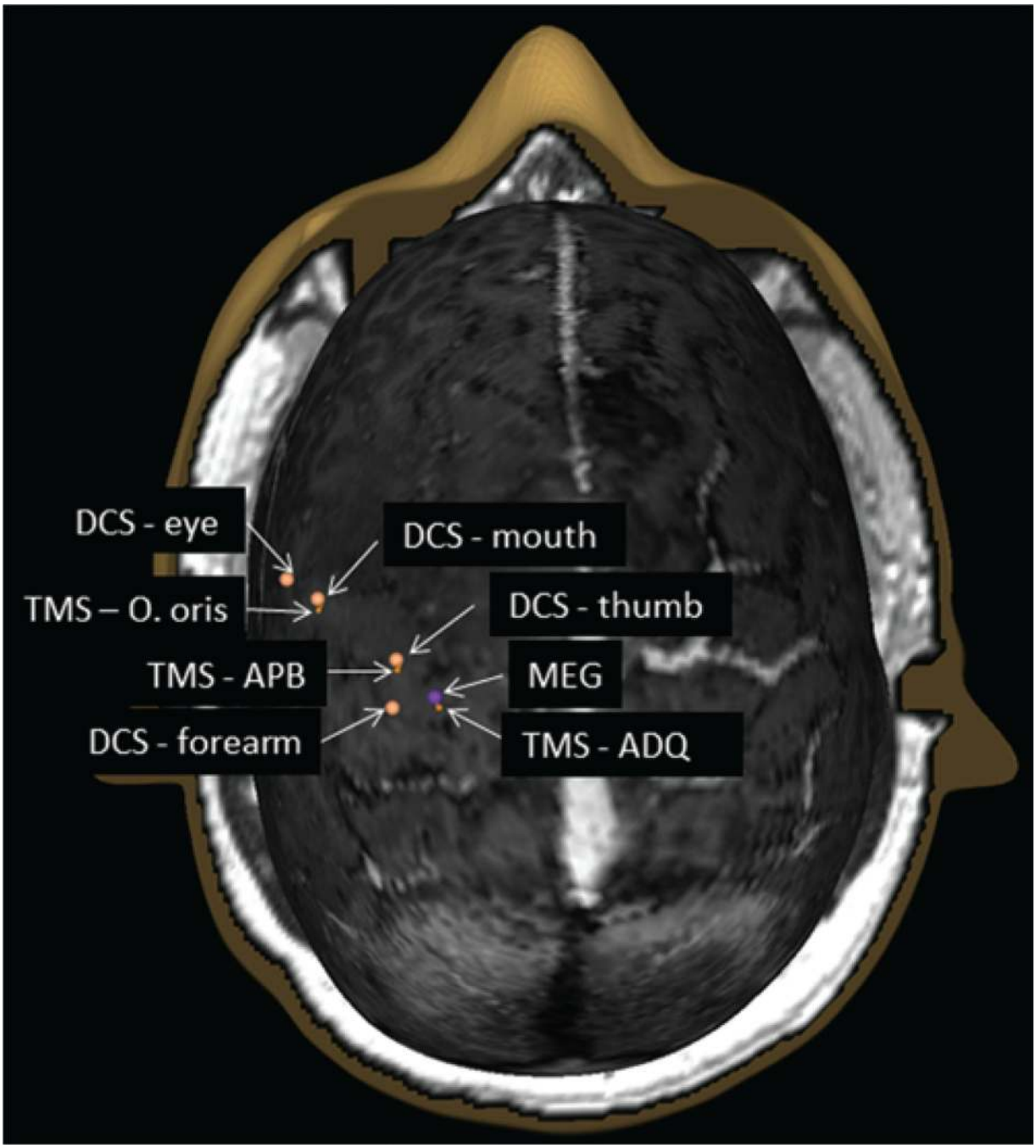

Fig. 3.

Example of a multimodal motor map showing MEG imaging *(purple sphere)*, TMS *(orange pins)*, and DCS *(orange spheres)* sites overlaid. ADQ = abductor digiti quinti; APB = abductor pollicis brevis; O. oris = orbicularis oris.

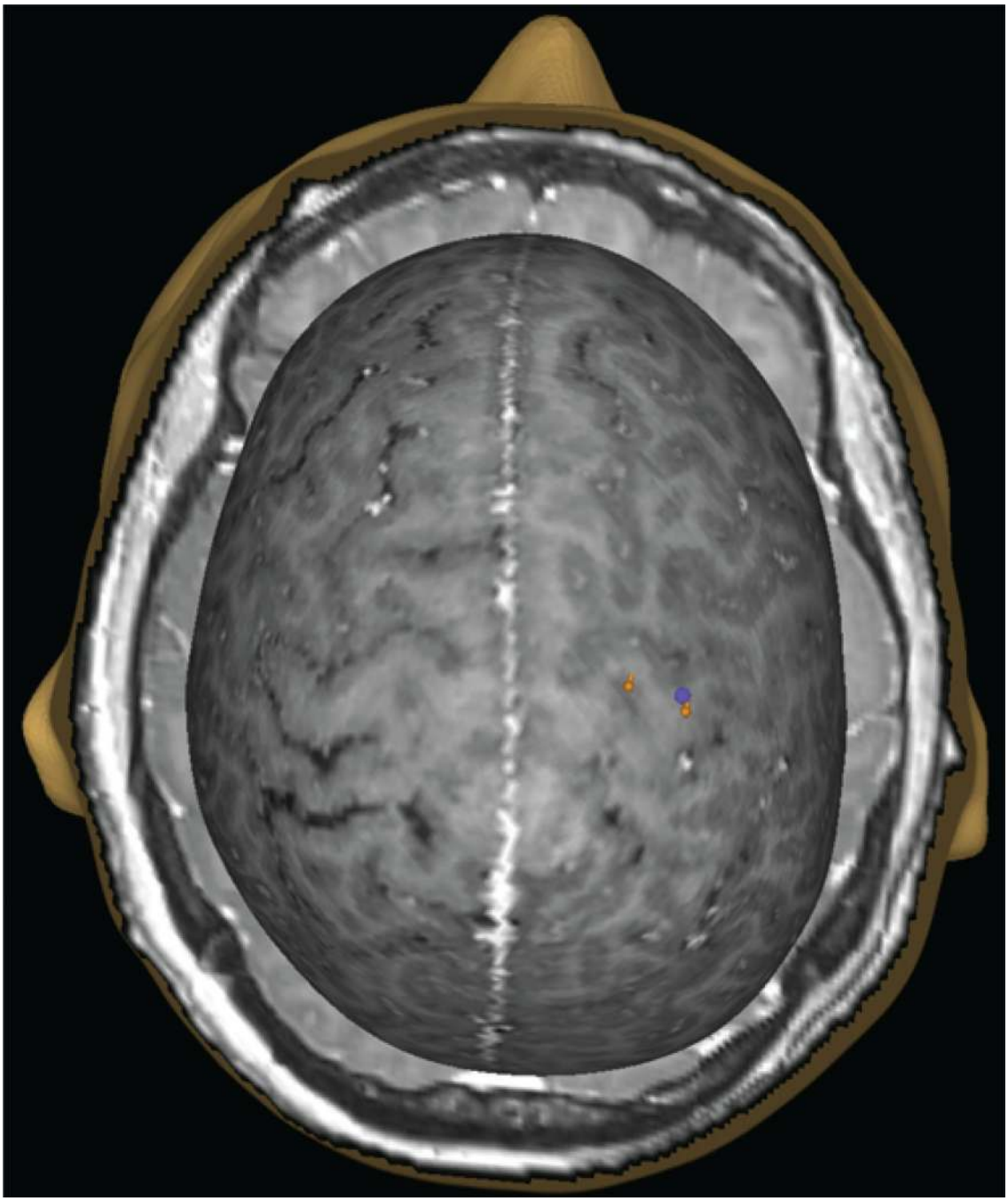

Fig. 4.

Example of a bimodal motor map with MEG imaging *(purple sphere)* and TMS *(orange pins)* sites overlaid. This patient had a negative motor map using DCS.

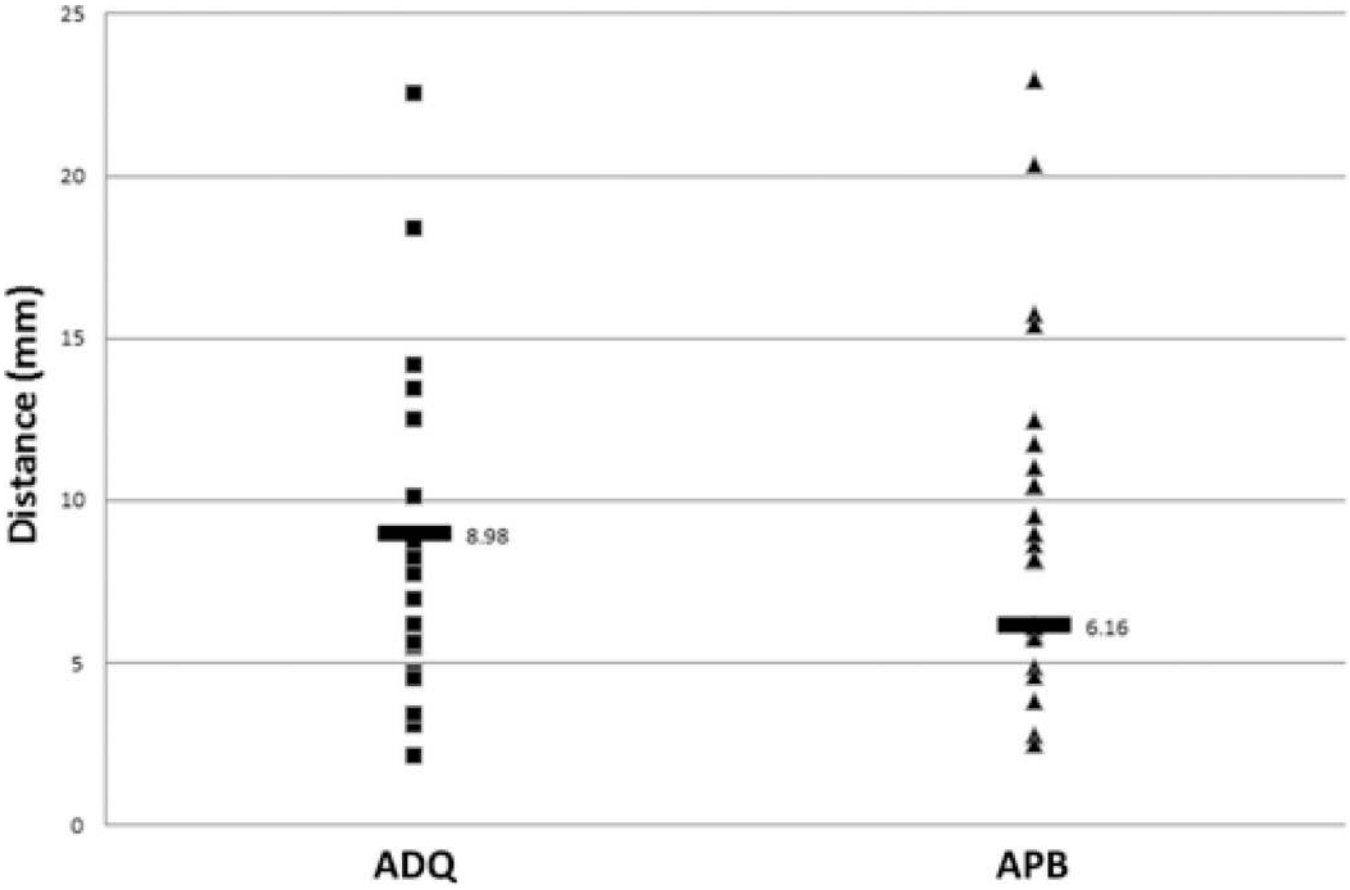

Fig. 5.

Scatterplot of distances from MEG imaging of the index finger motor site to TMS of the abductor digiti quinti and abductor pollicis brevis motor sites. The labeled *horizontal bar* in each series represents the median distance.

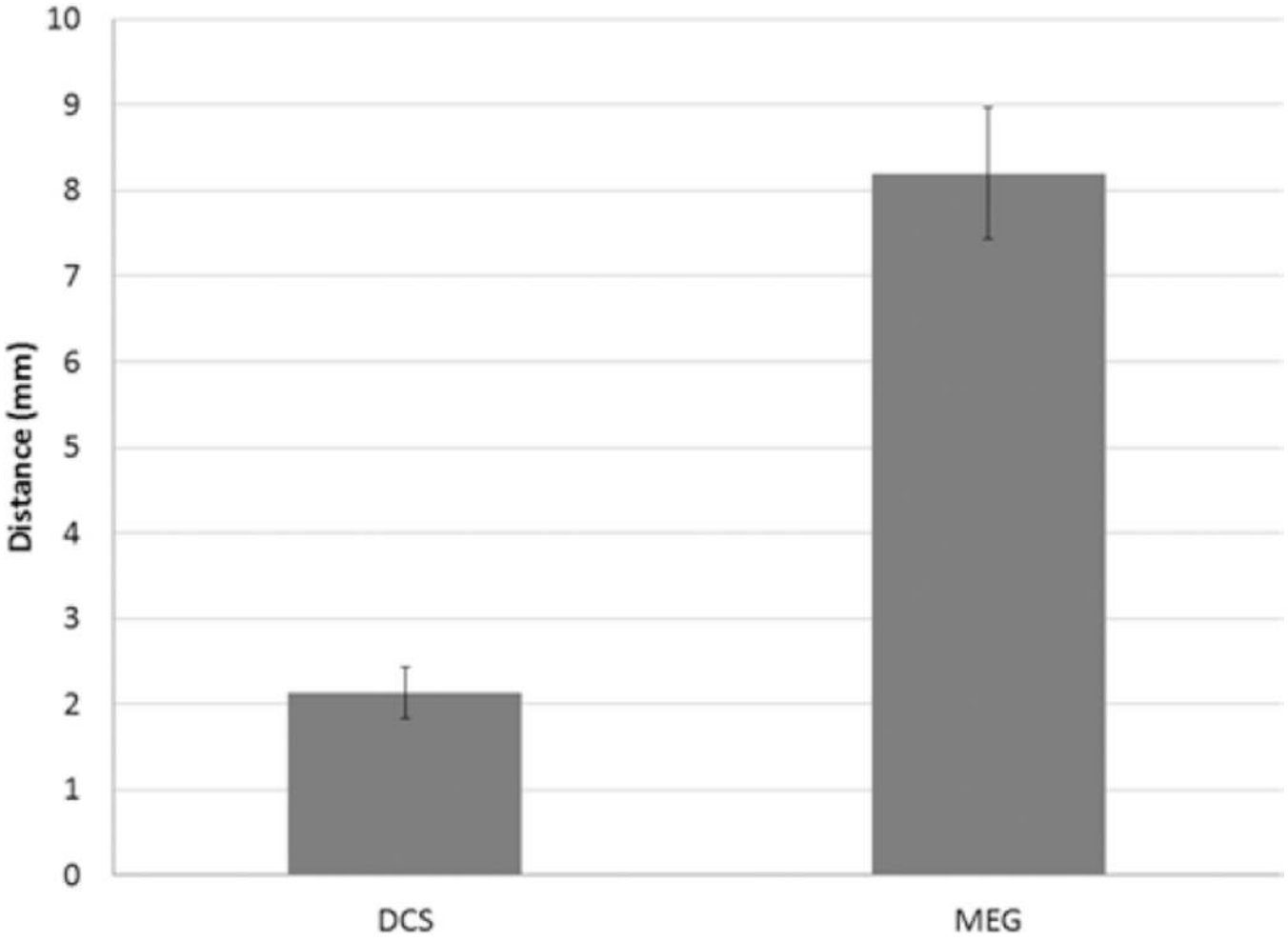

Fig. 6.

Bar graph showing the median distance from TMS motor sites (aggregated abductor digiti quinti and abductor pollicis brevis data) to corresponding DCS motor sites and to MEG imaging index finger motor sites (*error bar* = 95% CI).

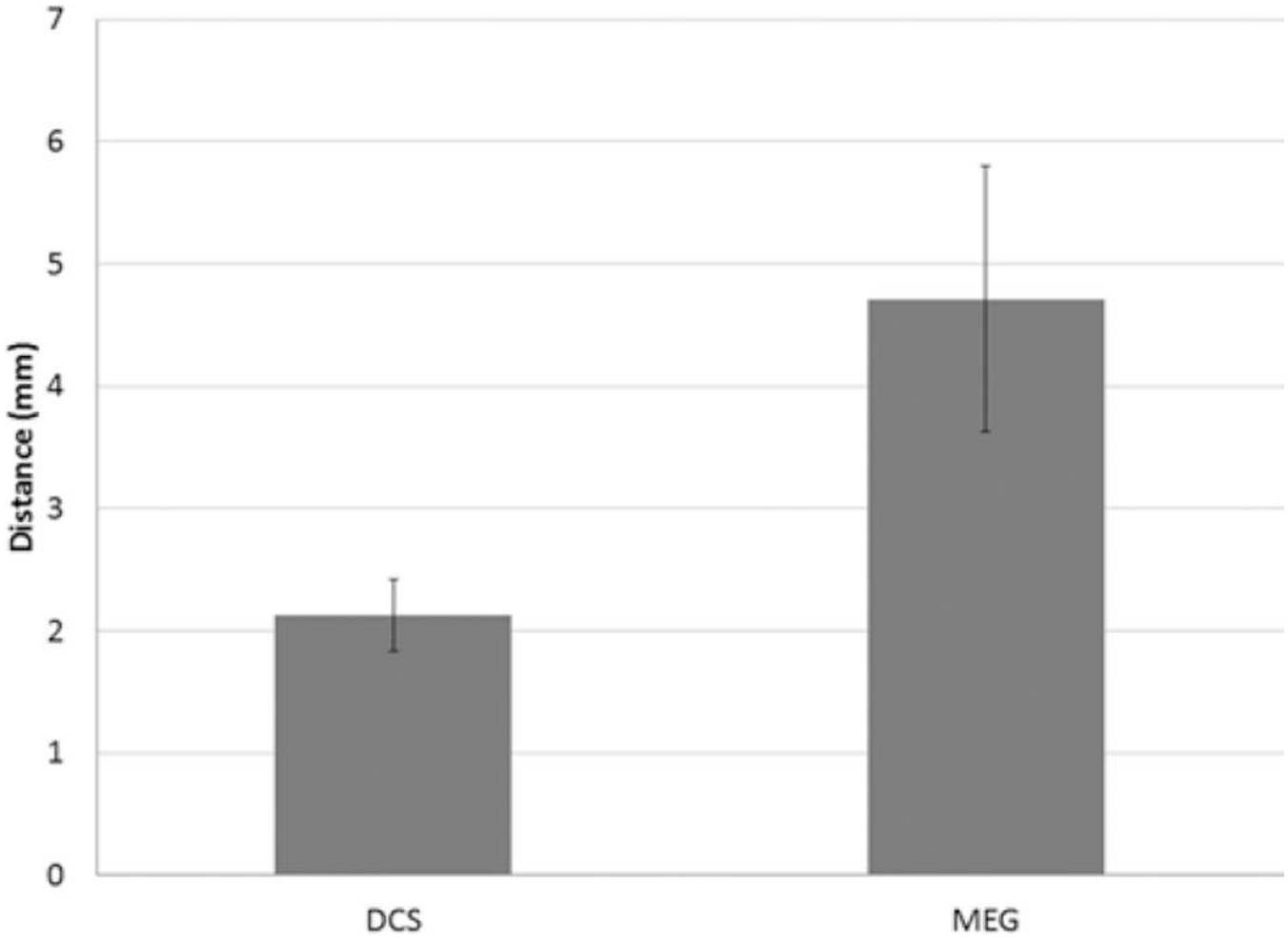

Fig. 7.

Bar graph showing the median distance from interpolated TMS motor sites (midpoint of abductor digiti quinti and abductor pollicis brevis muscles) to corresponding DCS motor sites and to MEG imaging index finger motor sites (*error bar* = 95% CI).

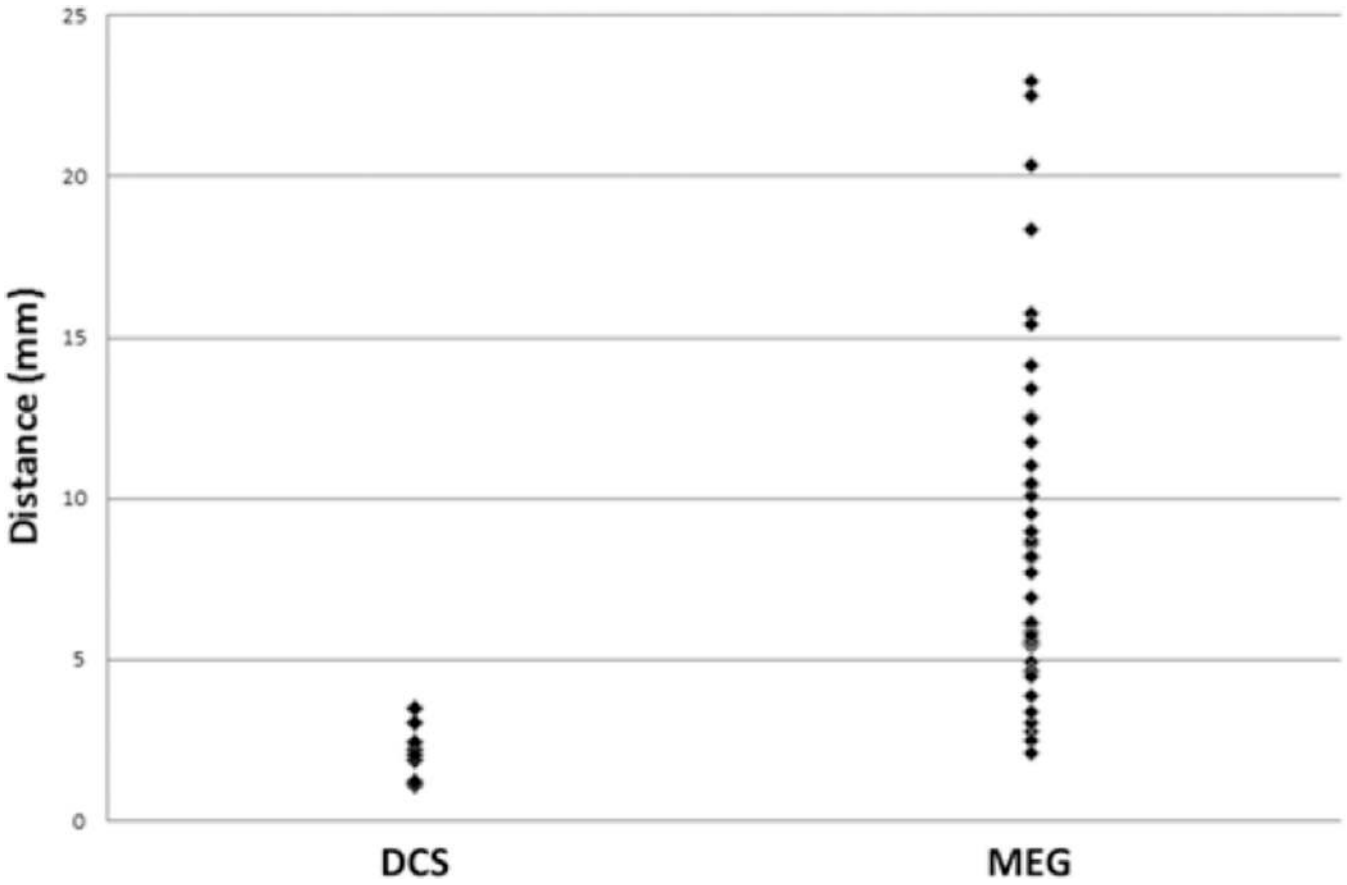

Fig. 8.

Scatterplot of distances from TMS motor sites to corresponding DCS motor sites and to MEG imaging index finger motor sites.

TABLE 1

Patient demographics and clinical characteristics*

Age (yrs) Sex	Laterality	Location	Recurrence	Pathology	WHO Grade	Postop Deficit
59, M	lt	temporal	yes	oligodendroglioma	III	none
39, F	lt	parietal	no	anaplastic astrocytoma	III	none
27, M	lt	frontal	no	anaplastic astrocytoma	III	none
36, F	lt	parietal	no	anaplastic astrocytoma	III	none
41, F	rt	frontal	no	oligodendroglioma	III	none
69, M	lt	frontal/insular	yes	glioblastoma	IV	none
68, M	lt	temporal	no	glioblastoma	IV	none
54, F	rt	parietal	yes	glioblastoma	IV	none
62, M	lt	temporal	yes	glioblastoma	IV	none
47, F	rt	frontal	no	oligodendroglioma	II	RUE paresis (transient)
40, F	lt	frontal/parietal	no	glioblastoma	IV	rt arm 4/5 strength, RUE apraxia
31, F	lt	frontal	yes	glioblastoma	IV	none
30, F	lt	frontal/temporal	no	anaplastic astrocytoma	III	none
70, M	lt	frontal	yes	glioblastoma	IV	none
46, F	rt	frontal	yes	treatment effect	none	none
67, M	lt	temporal	yes	oligodendroglioma	III	none
42, M	lt	temporal	yes	oligoastrocytoma	II	none
30, M	lt	frontal/temporal/insular	no	oligoastrocytoma	II	none
32, F	lt	parietal	no	oligodendroglioma	II	RUE apraxia (transient)
39, F	lt	parietal	no	oligoastrocytoma	II	none
46, F	rt	temporal	yes	oligodendroglioma	III	none
32, M	lt	temporal	no	oligodendroglioma	II	none
41, F	lt	frontal	yes	oligoastrocytoma	II	none
32, F	rt	frontal	yes	oligoastrocytoma	II	none

*RUE = right upper extremity.

TABLE 2

Comparison of distances (± SEM) between modalities

Modality	TMS (mm)	MEG Imaging (mm)
MEG imaging	4.71 ± 1.08	not applicable
DCS	2.13 ± 0.29	12.1 ± 8.2